Makara Journal of Technology

Volume 24 | Issue 3 Article 1

12-3-2020

A Density Functional Theory Study on using Montmorillonite to Reduce Air Pollution

Triati Dewi Kencana Wungu
Nuclear Physics and Biophysics Research Group, Department of Physics, Faculty of Mathematics and Natural Sciences, Institut Teknologi Bandung, Bandung 40132, Indonesia, triati@fi.itb.ac.id

Meqorry Yusfi
Instrumentation and Computational Physics Research Group, Department of Physics, Faculty of Mathematics and Natural Sciences, Institut Teknologi Bandung, Bandung 40132, Indonesia

Suprijadi Suprijadi
Research Center for Nanosciences and Nanotechnology, Institut Teknologi Bandung, Bandung 40132, Indonesia

Recommended Citation

Wungu, Triati Dewi Kencana; Yusfi, Meqorry; and Suprijadi, Suprijadi (2020) "A Density Functional Theory Study on using Montmorillonite to Reduce Air Pollution," *Makara Journal of Technology*: Vol. 24: Iss. 3, Article 1.
DOI: 10.7454/mst.v24i3.3592
Available at: https://scholarhub.ui.ac.id/mjt/vol24/iss3/1

Makara J. Technol. 24/3 (2020), 99–105
doi: 10.7454/mst.v24i3.3592

A Density Functional Theory Study on using Montmorillonite to Reduce Air Pollution

Triati Dewi Kencana Wungu[1,3*], Meqorry Yusfi[2], and Suprijadi[2,3]

1. Nuclear Physics and Biophysics Research Group, Department of Physics, Faculty of Mathematics and Natural Sciences, Institut Teknologi Bandung, Bandung 40132, Indonesia
2. Instrumentation and Computational Physics Research Group, Department of Physics, Faculty of Mathematics and Natural Sciences, Institut Teknologi Bandung, Bandung 40132, Indonesia
3. Research Center for Nanosciences and Nanotechnology, Institut Teknologi Bandung, Bandung 40132, Indonesia

[*]*E-mail: triati@fi.itb.ac.id*

Abstract

In this study, density functional theory (DFT) method is used to investigate the possibility of using a smectite clay mineral called montmorillonite (MMT) in reducing heavy metals, such as Cd, through Cd adsorption. The mechanism of Cd adsorption in MMT is observed theoretically, and the tetrahedrally isomorphic substitution on the upper layer of MMT is considered to observe the role of Al and Fe in strengthening Cd adsorption. Two types of MMT are modeled in this study: Al-MMT and Fe-MMT. The Al-MMT means that Al substitutes one atom in the upper tetrahedral layer of MMT, while Fe-MMT means that Fe substitutes one atom in the upper tetrahedral layer of MMT. According to the DFT calculation, Cd is adsorbed relatively strongly to Al-MMT compared with Fe-MMT, with Cd adsorption energy of –4.55 eV and –2.43 eV for Al-MMT and Fe-MMT, respectively. The density-of-state analysis shows that Cd helps reduce the gap between the highest valence-band energy and lowest conduction-band energy of Al-MMT and Fe-MMT. Thus, Cd/Al-MMT and Cd/Fe-MMT behave in a manner similar to a semiconductor.

Abstrak

Suatu Kajian Teori Fungsional Kerapatan tentang Penggunaan Monmorilonit untuk Mengurangi Polusi Udara. Dalam penelitian ini metode *density functional theory* (DFT) digunakan untuk meneliti kemungkinan mineral lempung smektit, yang disebut montmorillonit (MMT), untuk mereduksi logam berat seperti Cd melalui penyerapan Cd. Mekanisme penyerapan Cd dalam MMT diamati secara teoritis dan substitusi isomorfik tetrahedral di lapisan atas MMT dilakukan untuk melihat bagaimana peran Al dan Fe dalam memperkuat adsorpsi Cd. Ada dua jenis MMT yang dimodelkan dalam penelitian ini yaitu model Al-MMT dan Fe-MMT. Pada model Al-MMT, substitusi Al dilakukan pada lapisan tetrahedral atas MMT, sedangkan pada model Fe-MMT maka Fe menggantikan salah satu atom dalam lapisan tetrahedral atas MMT. Dari perhitungan DFT diperoleh bahwa adsoprsi Cd pada Al-MMT relative lebih kuat dibandingkan dengan Fe-MMT. Hal ini dapat dilihat dari energi adsorpsi Cd pada Al-MMT sebesar -4.55 eV dan pada Fe-MMT sebesar -2.43 eV. Hasil analisis *density of states* menunjukkan bahwa Cd memberikan kontribusi terhadap penyempitan band gap antara pita valensi maksimum dan pita konduksi minimum. Oleh karena itu, Cd/Al-MMT dan Cd/Fe-MMT menunjukkan perilaku seperti semikonduktor.

Keywords: DFT, montmorillonite, Cd

1. Introduction

Increasing economic growth often spurs the development of the automotive industry, thereby resulting in negative effects, especially on the environment. Air pollution caused by heavy metal from vehicle exhaust is worsening and tends to cause various diseases. Pollution also exposes people to carcinogenic and non-carcinogenic health risks [1]-[7].

Cadmium (Cd) is one of the heavy metal toxins produced mostly from engine oil consumption, mining, and metallurgy. Emissions of Cd to the environment are transported through air, water, and soil. Furthermore,

humans can be exposed to Cd through drinking water, food crops grown in contaminated soil, inhaled aerosol particles, and dust [8], [9].

In response to growing public concern regarding the health risks caused by Cd toxicity in humans, we need to consider methods to reduce environmental damage. Many studies have successfully applied technology and material science to solve environmental problems. Some researchers have used composite magnetite–chitosan microparticles [10], ZnS nanoparticles [11], and graphene oxide-supported organo-montmorillonite (MMT) composites [12] to remove Cd from a contaminated solution. The addition of nanobiochar [13] and functionalized MMT clay [14]-[16] was also reported to be an effective way to remove Cd in contaminated soil because those materials have a large surface area and can immobilize Cd through sorption. The adsorption mechanism of heavy metals on MMT is dependent on affinity sites on the clay [17]. In some cases, Cd preferentially binds to higher affinity components [18]. In addition, the adsorption of Cd increases with increasing soil solution pH, and acid activation influences MMT [19].

As MMT has a high capacity for cation exchange and adsorption of polar molecules in the interlamellar space, a number of studies have investigated the feasibility of utilizing MMT to further improve the removal of heavy metal or hazardous material through experimental and theoretical methods [20]-[25]. Adraa *et al.* [22] observed that all cations, including Cd, are strongly bonded to the composites of cysteine–MMT but this is not the case for the pristine clay mineral MMT. Therefore, in this study, modification of MMT is proposed through isomorphic substitution on its surface MMT to determine whether Cd can strongly adsorb to the MMT surface. Al and Fe are considered in isomorphic substitution on the surface of MMT. Therefore, this study focuses on examining the role of Fe and Al and the mechanism of Cd adsorption on the surface of MMT from the perspective of atomic scale.

2. Calculation Method

All electronic properties are calculated using density functional theory (DFT) method, as implemented in the Vienna Ab Initio Simulation Package [26], [27]. The generalized gradient approximations with Perdew–Burke–Ernzerhof function [28] is used for exchange-correlation energy. The projector augmented wave method for modeling core electrons is employed with an energy cutoff of 520 eV. The k-point mesh of 5 × 5 × 1 is generated by the Monkhorst–Pack method [29].

The adsorption energy of Cd on Al-substituted MMT and Fe-substituted MMT, E(ads), is calculated as follows:

$$E(ads) = E(Cd/Al\text{-}MMT) - [E(Cd) + E(Al\text{-}MMT)],$$
$$E(ads) = E(Cd/Fe\text{-}MMT) - [E(Cd) + E(Fe\text{-}MMT)],$$

where E(Cd/Al-MMT), E(Cd/Fe-MMT), E(Cd), E(Al-MMT), and E(Fe-MMT) correspond to the total energy of the Cd/Al-MMT system, total energy of the Cd/Fe-MMT system, total energy of isolated Cd, total energy of Al-MMT, and total energy of Fe-MMT, respectively.

3. Structural Simulation Model

MMT is a lamellar clay with a structure that mimics that of pyrophyllite (Figure 1), where the octahedral aluminum hydroxide ($Al(OH)_2$) sheet is sandwiched between two silicate (SiO_4) tetrahedral sheets. To avoid periodic image, we set the interlayer distance large enough at approximately 12 Å. Specifically, the distance between the basal atoms of oxygen on the basal tetrahedral sheet to the basal atom of oxygen on the next basal tetrahedral sheet is 18.66 Å.

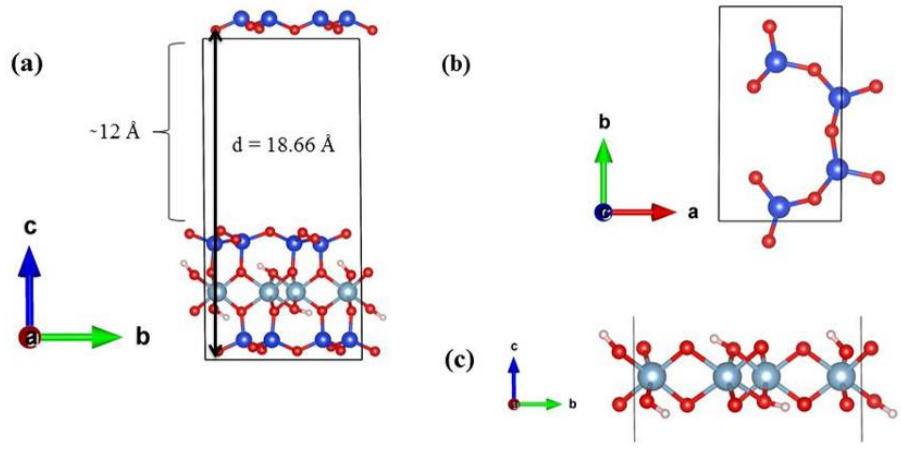

Figure 1. Structure of a Unit Cell of Pyrophyllite: (a) Side View, (b) Top View of Upper Silicate Tetrahedral Sheet, and (c) Side View of Octahedral Sheet

In nature, some minerals are present in MMT layers; thus, modifying the pyrophyllite structure through substitution in its layer is conducted to generate the MMT structure. In the octahedral sheet of the MMT structure, one aluminum (Al) atom of alumino-hydroxide is substituted by one magnesium (Mg) atom (Figure 2). The basal of the tetrahedral sheet is unmodified and the upper tetrahedral sheet is substituted by an aluminum/iron (Al/Fe) atom (Figure 3). Those substitutions result in a net negative charge that can attract the cation of polar molecules.

The Al/Fe site in the upper silicate (SiO_4) tetrahedral sheet of MMT is chosen based on the most stable configuration. Four possible MMT configurations are in each possible Al/Fe site. The configuration of Al/Fe site is shown in Figure 3. The Al/Fe replaces one of the Si atoms in site no. 1 for the first configuration, in site no. 2 for the second configuration, in site no. 3 for the third configuration, and in site no. 4 for the fourth configuration. Based on the minimum relative energy (Figure 4), the most stable Al-MMT and Fe-MMT structures are observed when Al is located in the third site and Fe in the second site. Figure 5 shows the most stable configurations of Fe-MMT and Al-MMT.

To observe the Cd adsorption on the Al-MMT and Fe-MMT structures, we determined the possibilities of Cd sites by scanning their position on top of the MMT surface in the *x* and *y* coordinates. The initial distance of Cd to the MMT surface is fixed (z coordinate is set at 0.5 in a fraction coordinate), whereas the x and y coordinates vary from 0.1 to 0.9 (in a fraction coordinate). The local minimum energy of Cd/Al-MMT and Cd/Fe-MMT obtained from the static calculation is shown in Figures 6 and 7, respectively. As presented in Figure 6, the local minimum energy is mainly observed at x = 0.3 and x = 0.8. Similar results are also observed in the case of Cd/Fe-MMT (see Figure 7).

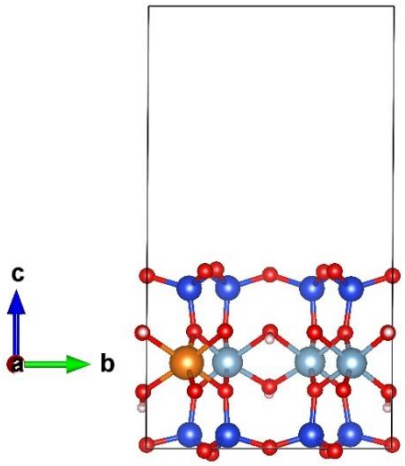

Figure 2. A Unit Cell of MMT. The Mg Atom (Brown Color) Substitutes for One of the Al Atoms in the Octahedral $Al(OH)_2$ Sheet

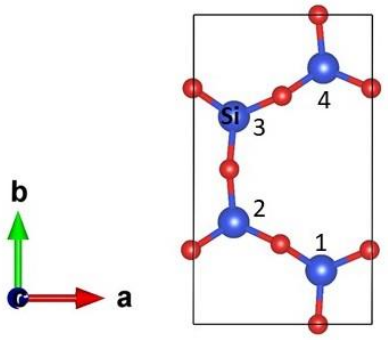

Figure 3. Top View of Upper Silicate (SiO4) Tetrahedral Sheets of MMT. Nos. 1, 2, 3, and 4 Correspond to Substitution Sites for Al or Fe

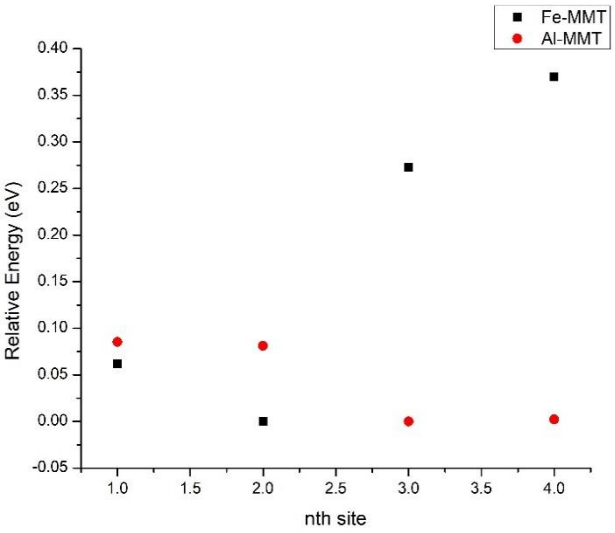

Figure 4. Relative Energy of Four Possible Configurations of Fe-MMT and Al-MMT

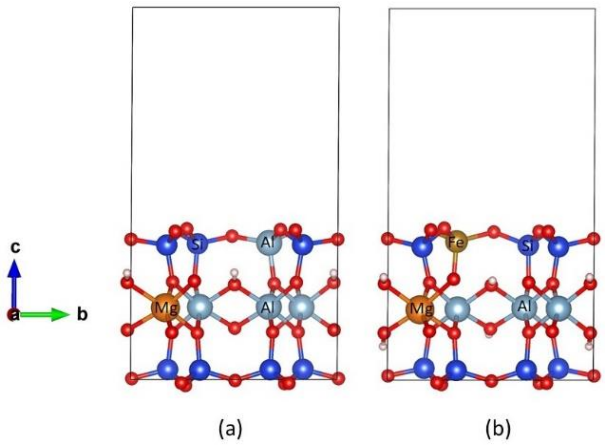

Figure 5. Optimized MMT Structures where (a) Al Substituted for the Upper Silicate Tetrahedral Sheet of MMT (Al-MMT) and (b) Fe Substituted for the Upper Silicate Tetrahedral Sheet of MMT (Fe-MMT)

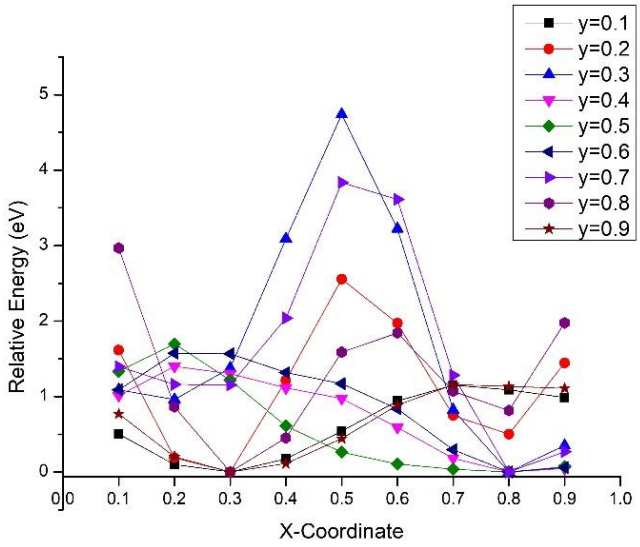

Figure 6. Relative Energy of Cd/Al-MMT for Varied x and y Coordinates. The z Coordinate is Fixed (z = 0.5). All Configurations are Performed Through Static Calculation

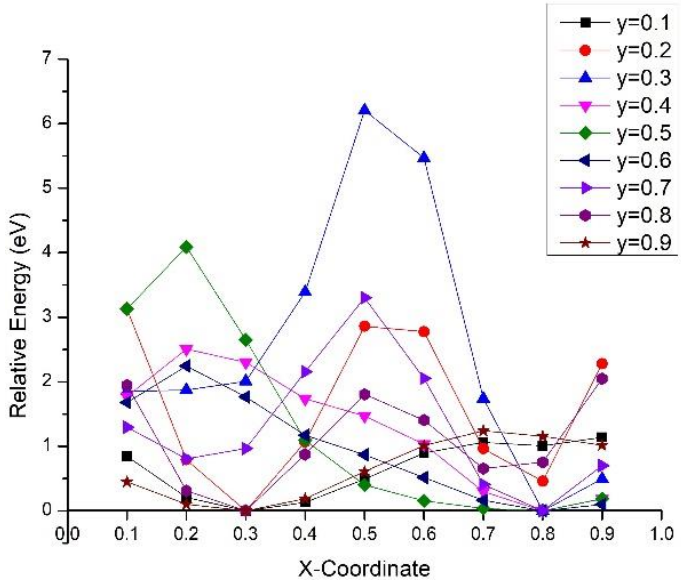

Figure 7. Relative Energy of Cd/Fe-MMT for Varied x and y Coordinates. The z Coordinate is Fixed (z = 0.5). All Configurations are Performed Through Static Calculation

Based on Figures 6 and 7, the next calculation aims to find the maximum global energy of Cd/Al-MMT and Cd/Fe-MMT through relaxation calculations. Nine initial configurations are obtained from the static calculation for each Cd/Al-MMT and Cd/Fe-MMT structure. Among those initial configurations, the minimum global energy is observed.

4. Results and Discussion

From the relaxation calculation, we found that the Cd atom is adsorbed on the cavity surface of Al-MMT (Figures 8a) and located near Al (Figure 8b). Figure 9 presents the optimized structure of Cd/Fe-MMT. Similar to the Cd/Al-MMT case, the Cd atom on the Cd/Fe-MMT is also adsorbed on the cavity surface of Fe-MMT (Figure 9a) and located near the Fe atom (Figure 9b). The Cd atom forms bonds with the three nearest neighboring oxygen atoms, which are O_1, O_2, and O_3. The Cd adsorption on the surface of the MMT structure changes certain bonds within the atoms. The stretching bond length within the Al-MMT and Fe-MMT structure due to the Cd adsorption is reported in Table 1.

The listed bond defined from the first row to the ninth row of Table 1 corresponds to the data of Al-MMT,

while the remaining rows correspond to the data of Fe-MMT. As shown in Table 1, the Al-O_1, Al-O_2, and Si-O_3 lengthen by 0.06, 0.03, and 0.06 Å, respectively, after Cd is adsorbed on the surface of Al-MMT. Although the Si-O_2 bond length does not change, the Al-O_2-Si angle enlarges to 1.05° due to the electron donation from Cd to O_2. In addition, the presence of Cd extends the distance between O_1 and O_3.

In the case of Fe-MMT, the Fe-O_2, Si-O_1, and Si-O_3 bond lengthens by 0.16, 0.06, and 0.06 Å, respectively, before the Cd is adsorbed on the surface of Fe-MMT. The Cd-O_2 bond length is also shorter than the Cd-O_1 bond length, as indicated by the enlargement of Fe-O_2-Si angle to 12°. Compared with the Fe-O_2-Si angle, the Si-O2-Si angle is enlarged only to 4°.

For the Al-O and the Fe-O bond length, the average is 1.79 Å and 1.9 Å, respectively, which is longer than the Si-O bond lengths, indicating that the Al-O and Fe-O bonds are weaker than the Si-O bond, as observed by Wang *et al*. [30]. Thus, the Al or Fe atoms seem to push forward O-promoting Cd-O bonds.

Comparing the bond length of Cd and O of the OH group (Cd-O_{OH}) in Cd/Al-MMT and Cd/Fe-MMT, we find that the O-O_{OH} bond length in Cd/Fe-MMT is longer

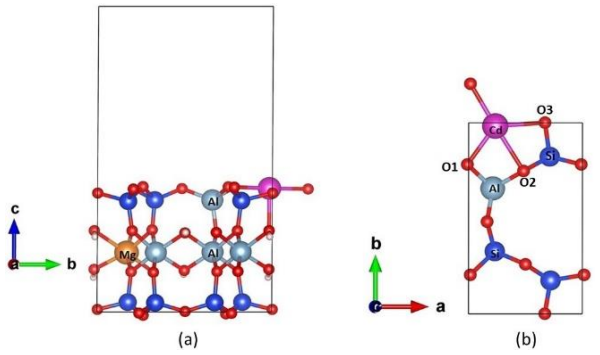

Figure 8. Optimized Structure of Cd/Al-MMT: (a) Side View and (b) Top View

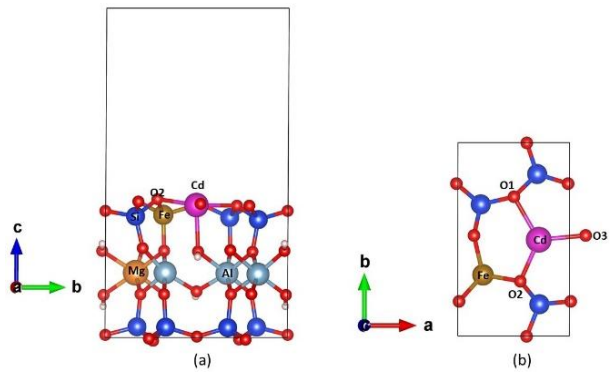

Figure 9. Optimized Structure of Cd/Fe-MMT: (a) Side View and (b) Top View.

Table 1. Bond Length Comparison Within MMT Atoms Before and After Cd Adsorption on Al-MMT and Fe-MMT Structure

Bond	Al-MMT		Fe-MMT	
	before	after	before	after
Al-O1	1.75 Å	1.81 Å		
Al-O2	1.73 Å	1.76 Å		
Si-O3	1.63 Å	1.69 Å		
Si-O2	1.61 Å	1.61 Å		
O1-O3	3.86 Å	4.14 Å		
Cd-O1	-	2.24 Å		
Cd-O2	-	2.51 Å		
Cd-O3	-	2.34 Å		
Cd-O_{OH}	-	2.27 Å		
Fe-O2			1.74 Å	1.90 Å
Si-O1			1.62 Å	1.68 Å
Si-O3			1.63 Å	1.69 Å
Cd-O1			-	2.33 Å
Cd-O2			-	2.16 Å
Cd-O3			-	2.23 Å
Cd-O_{OH}			-	2.31 Å

by 0.04 Å than that in Cd/Al-MMT. The reason is the large adsorption energy of Cd in Al-MMT. From the DFT calculation, the Cd adsorption energy on the Al-MMT and Fe-MMT is –4.55 eV and –2.43 eV, respectively. The optimized geometry structure and relative adsorption energies demonstrate a correlation between the distribution of the active surface groups, as identified by Liu *et al*. [31].

To observe how the electronic properties of Cd are adsorbed on Al-MMT and Fe-MMT, we present the total density of states (DOS). The DOS shows the existence of the energy state in a particular energy and determines that the energy state could be filled by an electron. When no state exists at a certain energy level, this energy state is always empty. Thus, if between the lowest energy state of the conduction band and the highest energy state of the valence band, the DOS is constantly zero, then an energy gap (E_g) exists between those energies. Based on E_g, the properties of the material can be defined. If E_g is zero, then the material behaves like a conductor. However, if E_g is not zero, then the material behaves like a semiconductor or an insulator depending on the width of E_g. In semiconductors, E_g is typically <3 eV and in insulators, >5 eV.

Figures 10 and 11 correspond to the total DOS of the Al-MMT and Cd/Al-MMT, respectively. As depicted in Figure 10, the DOS crosses the Fermi level, and E_g is zero, which makes the Al-MMT behave similar to a conductor/ferromagnetic metal. However, as shown in Figure 11, no DOS crosses the Fermi level, and E_g is 2.6 eV. Thus, the Cd/Al-MMT behaves like a semiconductor. Based on this finding, the addition of Cd to the Al-MMT changes the electronic properties of Al-MMT from conductor to semiconductor with bandgap of 2.6 eV. The occurrence of the Cd atom in the Al-MMT shifts the DOS to the lower energy so that it is below the Fermi level. Furthermore, the localized state in the conduction band at the energy range of 2.6–3 eV appeared after Cd adsorption.

Figures 12 and 13 show the total DOS of Fe-MMT and Cd/Fe-MMT, respectively. As depicted in Figure 12, the E_g of the DOS of spin-up is zero while that of spin-down is approximately 0.6 eV. Therefore, the Fe-MMT behaves in a half-metallic manner because the DOS of spin-up exhibits metallic-like behavior while the DOS of spin-down presents a semiconductor-like behavior. The addition of Cd to Fe-MMT shifted the DOS of spin-up to the lower energy and created a higher bandgap at 1.06 eV (Figure 13). Thus, Cd/Fe-MMT has a semiconductor-like behavior, which is similar to that of Cd/Al-MMT. The preceding DOS analysis shows that Cd plays a role in reducing the energy gap between the highest valence-band energy and the lowest conduction-band energy of each Al-MMT and Fe-MMT. The change of the electronic properties of Al-MMT and Fe-MMT describes the Cd adsorption mechanism on Al-MMT and Fe-MMT. Furthermore, based on the adsorption energy analysis, the Cd adsorption on Al-MMT is stronger than that in Fe-MMT. The DOS analysis can confirm the energy result of Cd adsorption.

The large E_g in Cd/Al-MMT indicates that the minimum energy needed to excite an electron to the conduction band is higher than that in Cd/Fe-MMT.

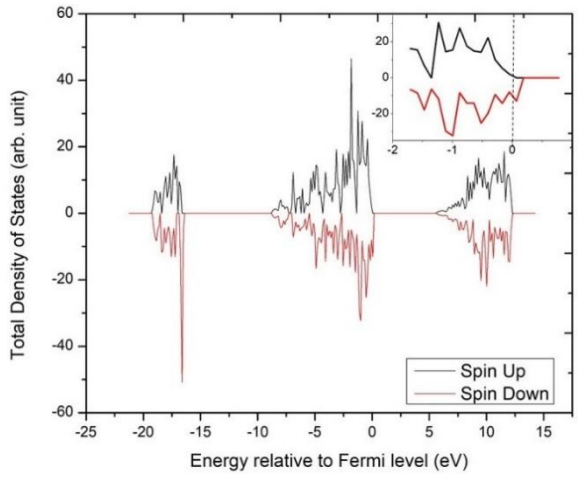

Figure 10. Total DOS of Al-MMT. The Fermi Level is Set to Zero Axis

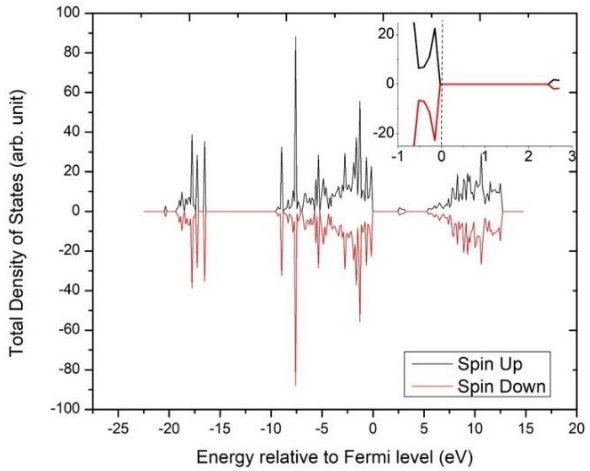

Figure 11. Total DOS of Cd/Al-MMT. The Fermi Level is Set to Zero Axis

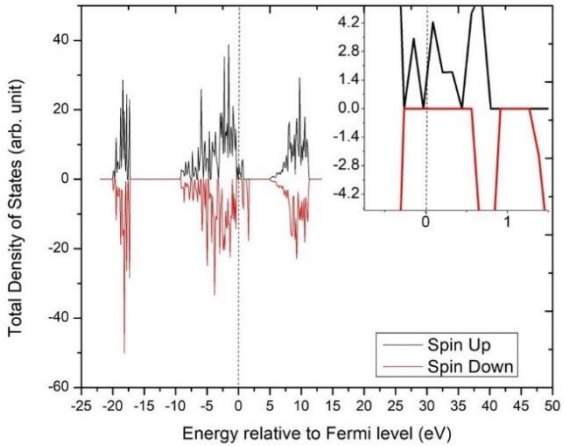

Figure 12. Total DOS of Fe-MMT. The Fermi Level is Set to Zero Axis

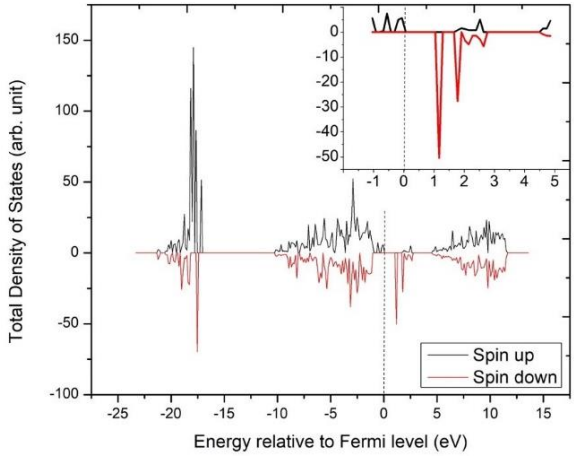

Figure 13. Total DOS of Cd/Fe-MMT. The Fermi Level is Set to Zero Axis

Our calculation shows that MMT can be used as a material to remove heavy metal, such as Cd, through binding interaction with the silicate of MMT. The isomorphic substitution in the tetrahedral of MMT (silicate layer) by Al or Fe plays an important role in strengthening the Cd-binding interaction with the surface of MMT.

5. Summary

The adsorption of Cd on Al-MMT and Fe-MMT were conducted through DFT. The DFT calculation results show that Cd is adsorbed more stably to Al-MMT than to Fe-MMT based on Cd adsorption energy. The DOS analysis shows that Cd plays a role in reducing the highest valence-band energy and lowest conduction-band energy of the Cd/Al-MMT and Cd/Fe-MMT structures. The electronic properties of Cd/Al-MMT and Cd/Fe-MMT show the semiconductor-like behavior with a different bandgap.

Acknowledgements

Part of this study was conducted with financial support from Penelitian Unggulan Perguruan Tinggi 2017, Riset Inovasi KK ITB 2017, and Penelitian Dasar Unggulan Perguruan Tinggi research scheme. All calculations were partly performed at the Advanced Computing Laboratory of the Department of Physics and the Research Center for Nanosciences and Nanotechnology, Institut Teknologi Bandung.

References

[1] A.A. Mohammadi, A. Zarei, S. Majidi, A. Ghaderpoury, Y. Hashempour, M.H. Saghi, A. Alinejad, M. Yousefi, N. Hosseingholizadeh, M. Ghaderpoori, MethodsX. 6 (2019) 1642.
[2] J.Y. Chung, S.D. Yu, Y.S. Hong, J. Prev. Med. Pub. Health. 47 (2014) 253.
[3] H.I. Afridi, T.G. Kazi, M.K. Jamali, G.H. Kazi, M. B. Arain, N. Jalbani, G.Q. Shar, Spectrosc. Lett. 39 (2006) 203.
[4] D.C. Bellinger, Birth Defects Research Part A - Clin. Mol. Teratology. 73 (2005) 409.
[5] T. Inaba, E. Kobayashi, Y. Suwazono, M. Uetani, M. Oishi, H. Nakagawa, K. Nogawa, Toxicol. Lett. 159 (2005) 192.
[6] L. Järup, M. Berglund, C.G. Elinder, G. Nordberg, M. Vahter, Scand. J. Work Environ. Health. 24 (1998) 1.
[7] D. Beyersmann, A. Hartwig, Arch. Toxicol. 82 (2008) 493.
[8] M.D. Somoano, M.E. Kylander, M.A. López-Antón, I. Suárez-Ruiz, M.R. Martínez-Tarazona, M. Ferrat, B. Kober, D.J. Weiss, Environ. Sci. Technol. 43 (2009) 1078.
[9] P. Xu, Y. Chen, S. He, W. Chen, L. Wu, D. Xu, Z. Chen, X. Wang, X. Lou, Chemosphere. 246 (2020) 125777.
[10] M.F. Hamza, Y. Wei, A. Benettayeb, X. Wang, E. Guibal, J. Mater. Sci. 55 (2020) 4193.
[11] C. Wang, H. Yin, L. Bi, J. Su, M. Zhang, T. Lyu, M. Cooper, G. Pan, J. Hazard. Mater. 384 (2020) 121461.
[12] J. Wei, M.F.A. Aboud, I. Shakir, Z. Tong, Y. Xu, ACS Appl. Nano Mater. 3 (2020) 806.
[13] W. Liu, Y. Li, Y. Feng, J. Qiao, H. Zhao, J. Xie, Y. Fang, S. Shen, S. Liang, Sci. Rep. 10 (2020) 858.
[14] L. Wang, X. Li, D.C.W. Tsang, F. Jin, D. Hou, J. Hazard. Mater. 387 (2020) 122005.
[15] S. Yan, Y. Cai, H. Li, S. Song, L. Xia, Environ. Pollut. 252 (2019) 1509.
[16] Z.-X Chen, H.-R Zhu, Z.-J Zhou, Q.-X Zhao, J. Agr. Res. Environ. 36 (2019) 528.
[17] L. Mei, H. Tao, C. He, X. Xin, L. Liao, L. Wu, G. Lv, J. Nanomater. 2015 (2015) 925268.
[18] H. Du, W. Chen, P. Cai, X. Rong, K. Dai, C.L. Peacock, Q. Huang, Sci. Rep. 6 (2016) 19499.
[19] K.G. Bhattacharyya, S.S Gupta, Ind. Eng. Chem. Res. 46 (2007) 3734.
[20] E. Scholtzova, D. Tunega, J. Madejova, H. Palkova, P. Komadel, Vib. Spectrosc. 66 (2013) 123.
[21] C.F. Ferreira, S.H. Pulcinelli, L. Scolfaro, P.D. Borges, ACS Omega. 4 (2019) 14369.
[22] K.E. Adraa, T. Geordelin, J.-F. Lambert, F. Jaber, F. Tielens, M. Jaber, Chem. Eng. J. 314 (2017) 406.
[23] M.M. Wahba, A.M. Zaghloul, J. Appl. Sci. Res. 3 (2007) 421.
[24] T. Undabeytia, E. Morillo, C. Maqueda, Clay Miner. 31 (1996) 485.
[25] P. Stathi, I.T. Papadas, A. Tselepidou, Y. Deligiannakis, Global NEST J. 12 (2010) 248.
[26] G. Kresse, J. Hafner, Phys. Rev. B 48 (1998) 13115.
[27] G. Kresse, Furthm¨uller, Phys. Rev. B 54 (1996) 11169.
[28] J.P. Perdew, K. Burke, M. Ernzerhof, Phys. Rev. Lett. 77 (1996) 3865.
[29] H.J. Monkhorst, J.D. Pack, Phys. Rev. B 13 (1976) 5188.
[30] H. Wang, Y. Ji, J. Chen, G. Li, T. An, Sci. Rep. 5 (2015) 15059.
[31] X. Liu, X. Lu, E. J. Meijer, R. Wang, H. Zhou, Geochim. Cosmochim. Acta. 81 (2012) 56.